The crop residue conundrum: maintaining long-term soil organic carbon stocks while reinforcing the bioeconomy, compatible endeavors?

Christhel Andrade[1,2,*], Hugues Clivot[3], Ariane Albers[1], Ezequiel Zamora-Ledezma[4], Lorie Hamelin[1]

[1] Toulouse Biotechnology Institute (TBI), INSA, INRAE UMR792, and CNRS UMR5504, Federal University of Toulouse, 135 Avenue de Rangueil, F-31077, Toulouse, France.

[2] Department of Chemical, Biotechnological and Food Processes, Faculty of Mathematical, Physics and Chemistry Sciences. Universidad Técnica de Manabí (UTM), 130150 Portoviejo, Ecuador.

[3] Université de Reims Champagne Ardenne, INRAE, FARE, UMR A 614, 51097 Reims, France.

[4] Faculty of Agriculture Engineering. Universidad Técnica de Manabí (UTM), 13132 Lodana, Ecuador.

Supplementary Information 1 (SI1)

INDEX

1. Pedoclimatic data

The climate of France can be grouped into 8 typologies (Joly et al., 2010) as shown in Fig S1, while the soil texture of the agricultural lands can be defined as sandy, balanced, silty, or clayey (GisSol, 2011) according to Fig S2.

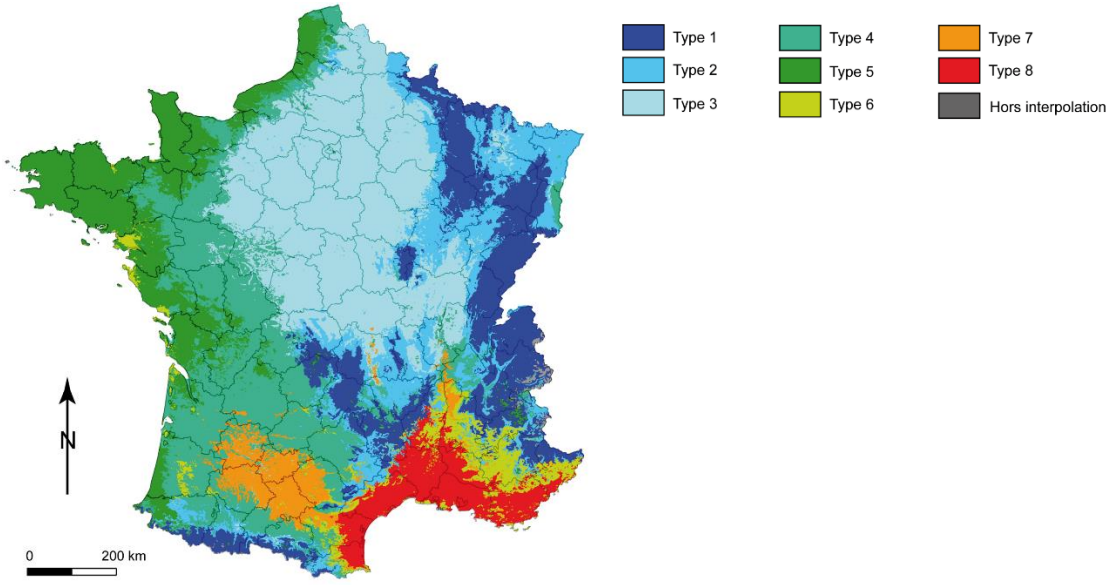

Fig S1. France climate typologies. Type 1: mountain climates, Type 2: the semi-continental climate and the climate of the mountain margins, Type 3: The degraded oceanic climate of the central and northern plains, Type 4: Altered oceanic climate, Type 5: The frank oceanic climate, Type 6: The altered Mediterranean climate, Type 7: The climate of the South-West Basin, Type 8: The frank Mediterranean climate, Hors interpolation: Out of interpolation. (Joly et al., 2010).

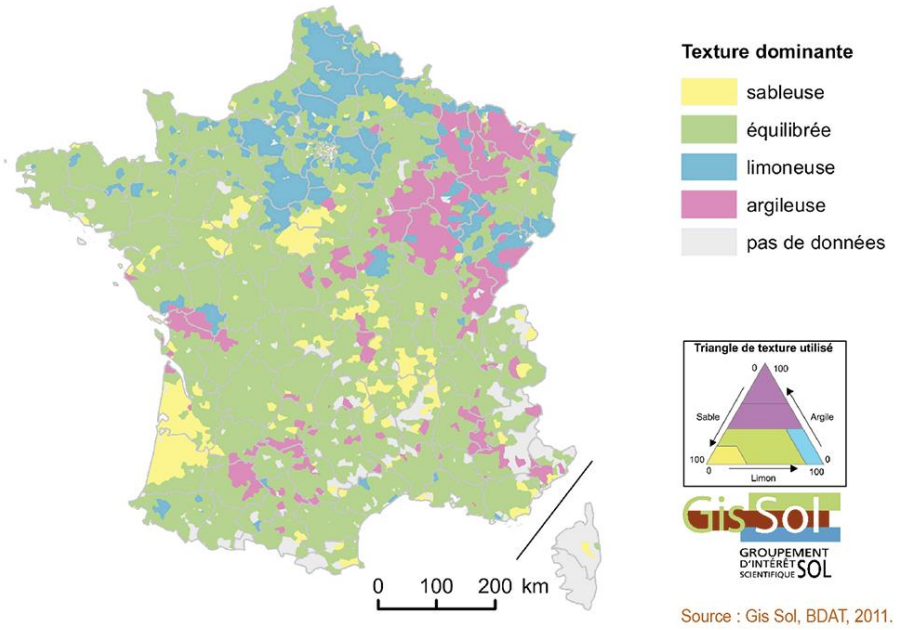

47

48 Fig S2. Dominant soil textures of the agricultural lands of France. Sableuse : sandy, équilibrée :
49 balanced, limoneuse : silty, argileuse : clayey, pas de données : no data. Retrieved from (GisSol,
50 2011).

51 The APCUs in Launay et al. (2021) were created using the SAFRAN grid while the climate data
52 input to the model in this work came from DRIAS RCP4.5, therefore some points of the grid
53 were lost during the adaptation. Besides, we used Launay et al. (2021) yields obtained from
54 STICS modeling, where some simulation units were lost during the modeling, thus no yields
55 were available for those units. Changing the climate grid and recycling the simulated yields are
56 major differences from Launay et al. (2021) and resulted in 11784 APCU and 60390 simulation
57 units in the present work vs 12060 APCU and 62694 simulation units in Launay et al. (2021).
58 This also affected the total area included in the study, which decrease from 18.35 Mha to
59 14.89 Mha at the APCU level, and from 4.79 Mha to 3.48 Mha at the simulation units level

60 **2. Crop rotations**

61 The crop rotations were retrieved from Launay et al., (2021). Due to the high resolution of the
62 data, a total of 1472 crop rotations were included (or 1588 if we considered the type of tillage

as a differentiation in the rotation). The crops included in the rotations are grain and silage maize, winter wheat, winter and spring peas, rapeseed, sunflower, and sugar beet. The crop rotations also included temporary grasslands, alfalfa, and cover crops (mustard and ray-grass). Temporary grasslands, alfalfa, and cover crops were not considered to be exported for bioeconomy because they are already being fully used for other purposes as animal bed and fodder (temporary grasslands and alfalfa) or are generally left on soils to maintain N levels (cover crops).

The original retrieved data included only 33 years of information, with rotation durations varying from 1 to 13 years. For the 100 years of modeling, we recycled the 33 years of original data. As a limitation of this work, the recycling of each 33 years meant that for some simulation units the rotations at year 33 were not completed but the following year 34 presented the crop corresponding to the first crop in the sequence.

The product yield of each crop depends on the pedoclimatic characteristics and farming management; therefore, it varies among simulation units. We obtained the spatially explicit yields from the STICS results modeled in Launay et al. (2021) and used the average value for the 30 years considered there. This means that for a given simulation unit, the grain yield in tonnes per ha of a given crop in the sequence will be the same throughout the 100 years of the modeling done in this work.

The total annual production of each crop (cover crops excluded) for the starting year 2020, as well as the technical harvestable fraction, are shown in Table S1.1. To determine the most representative crop in arable lands in France we determined the mean contribution of each crop for the whole mix of the considered crops for the 100 years' timeframe (Fig S3). The amount of crop residues currently exported is specific for each simulation unit and varies among the years according to the crop sequences. However, on average for the 100 years at a national scale 466656 tonnes grain ha^{-1} $y^{-}1$ (DM) are produced in the cropland surface included

in this study, of which 46% of the residues are already being used for animals. The dataset containing the crop sequences, annual yields, and information about the current exporting of the crop sequences per simulation unit and the scripts to determine the total annual yield per crop, annual crop contribution to the mix, and annual percentage of crops exported are available in https://doi.org/10.48531/JBRU.CALMIP/AUEEEJ. It must be noted that crops indicating current exports refer to a 100% exporting rate of the harvestable crop residue.

Table S1.1. Crop residues considered to be exported for bioeconomy and the technical harvestable fraction of the residues.

Crops included in this study	**Crop residue considered for bioeconomy**	**Estimated biomass potential for crop residue at national scale (Mtonnes y^{-1} DM)[a]**	**Technical harvestable fraction of residues**
Winter wheat[b]	YES	35.43	0.60
Grain maize	YES	14.15	0.70
Silage maize	NO	0.26	0
Protein peas[c]	YES	0.00	0.60
Rapeseed	YES	3.18	0.55
Sunflower	YES	0.89	0.80
Sugarbeet	YES	1.20	0.91
Alfalfa	NO	0.05	0
Temporary grasslands (English ryegrass)	NO	1.13	0
Potential biomass available for the bioeconomy[c]		**30.39**	

[a] Average yield for all the simulations units in the year 2021. The yields vary with the year due to the crop rotations;

[b] The crop rotations used here were the same as in Launay et al. (2021). They performed the SOC simulations using STICS and all the cereal-like crops (wheat, barley, oats, rice, etc.) were considered to be winter wheat. Since we

recycled the crop rotations, we also consider the ensemble of cereal-like crops to be winter wheat; [c] winter peas and spring peas are considered as protein peas in AMG, thus the total yield was calculated as a mixture of the two types of peas.

[c]Total crop residues considered for bioeconomy minus the fraction already exported for other services (46%).

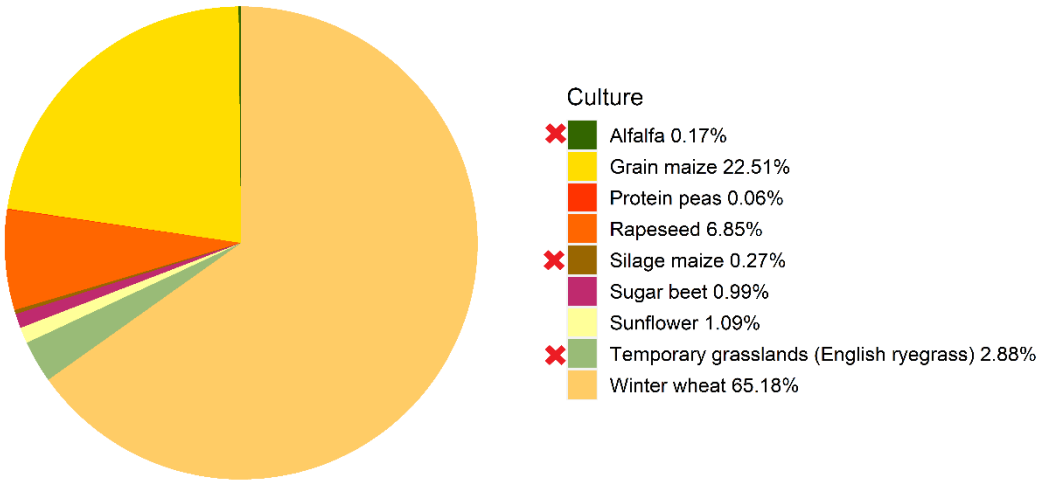

Biomass amount contribution per crop (average for 100 years)

Fig. S3. Contribution of each type of crop to the total residual biomass production (DM) in France (2020 – 2120 timeframe). Red x indicates crops not harvested in the bioeconomy scenarios.

3. Bioeconomy technologies

The conditions assumed for each considered technology are briefly explained in this section.

Pyrolysis: Pyrochar coproduct

Pyrolysis is a thermochemical process that converts the biomass to bio-oil at high temperatures in the absence of oxidants, with the coproduction of gas and biochar, henceforth referred to as pyrochar. The process can be classified as fast or slow pyrolysis. Fast pyrolysis comprises mid-range temperatures and low times (300-500°C, seconds to a few minutes), which enhance the production of bio-oil (75-50% bio-oil, 12-20% pyrochar, 20-40% gas) (Malyan et al., 2021). Slow pyrolysis is carried out at high temperatures and longer retention

times (500-700°C, minutes), favoring higher yields of pyrochar (30% bio-oil, 35% pyrochar) (Lehmann and Joseph, 2010). From an economic point of view (i.e., higher yield of bio-oil), we consider the use of the crop residues in a fast pyrolysis process.

Gasification: Gaschar coproduct

Gasification is a thermochemical process, which as opposed to pyrolysis, is carried out in presence of an oxidant agent. Gasification generates syngas and co-products, such as gaschar, tar, and ashes. Since gasification is carried out at higher temperatures than pyrolysis (700-1200°C), it has been noted that a lower amount of biochar is produced (10%) but of higher stability than that produced under pyrolysis processes (Molino et al., 2016). In this study, we considered a gasification process carried out at temperatures ranging from 800-1200°C, followed by the return of the resulting gaschar to the arable lands. We did not consider the tar (undesirable co-product) nor the ashes (high in silica and low in C) as EOM to the soil.

Hydrothermal Liquefaction: Hydrochar coproduct

Hydrothermal liquefaction (HTL) is a thermochemical process carried out at low temperatures of around 280-370°C with retention times of around 20-30 minutes. HTL uses wet biomass (15-20% dry matter) in contrast to pyrolysis and gasification, which require a pre-treatment to dry the matter to >90% (Jahirul et al., 2012). HTL produces bio-oil and a solid residue called "hydrochar". Note that there is a similar process called hydrothermal carbonization (HTC), in which the main product is hydrochar and not bio-oil. HTC processes involve higher temperatures (300-450°C) over a longer period comprising hours, making HTL hydrochar is constitutively different from HTC hydrochar. Catalysts can enhance the efficiency of HTL processes, especially alkali catalysts as K_2CO_3 (Seehar et al., 2021). We consider an HTL process at temperatures ranges of 300-400°C aided by catalysts with the hydrochar as EOM to soils.

Anaerobic Digestion: Digestate coproduct

In the anaerobic digestion (AD) process the organic constituents of the biomass are decomposed by microorganisms in the absence of oxygen. AD generates biogas, which is composed of methane, carbon dioxide, and traces of other gases, as well as a by-product known as digestate. AD uses a wide variety of biomass-based feedstock, which could be wet (15-35% DM) or dry (10%). The most common AD processes co-digest more than one substrate, at mesophilic temperatures (30-40°C) with retention times varying according to the feedstock (typically 10-25 days). The AD scenario of this study consists of a CR and manure (cattle, pig, and poultry) mixture, whereby the C return to the soil is computed from CR only.

Lignocellulosic ethanol: Molasses coproduct

Bioethanol is a biofuel produced from the fermentation of sugars in the biomass and its conversion into alcohol employing microorganisms (Swain et al., 2019). In this work, we consider that CR are exposed to an acid pretreatment that frees cellulose and hemicellulose, followed by the hydrolysis to glucose and xylose, which are fermented to ethanol by the action of *Saccharomyces cerevisiae*, and finally purified by distillation (Bušić et al., 2018). The unconverted fractions are directed to a residual stream known as stillage, which is centrifuged to separate the liquid fraction (molasses) and the solid fraction (Tonini et al., 2016). The solid fraction is normally used as an animal feed supplement and for energy production in power plants, therefore, here we only consider the return of the bioethanol molasses to the soils.

4. Carbon inputs from bioeconomy and AMGv2 adaption

Modifications were performed on AMGv2 to consider the input of the bioeconomy co-products as C sources in the soil.

2.1 Calculation of C inputs: Carbon conversion (Cc)

We define C conversion (Cc) as the percentage of initial C in the biomass that is present in the co-product. It is the mass of C in the solid co-product divided by the mass of C in the initial dry biomass (Eq S1).

$$\%Cc = \frac{BpY * BpC}{BmC} * 100 \qquad \text{(Eq S1)}$$

where Cc is the carbon conversion (%), BpY is the coproduct yield (kg Bp kg^{-1} biomass), which corresponds to the amount of coproduct resulting from the treatment of 1 kg of feedstock during the bioeconomy process, BpC is the carbon content in the co-product (kg C kg^{-1} Bp), and BmC is the initial carbon content in the biomass (kg C kg^{-1} biomass).

Andrade et al., reviewed the literature to determine the C pathway from crop residues to understand the amount of feedstock C that is present in each coproduct considered in this work. The study employed Eq S1 to determine the Cc coefficient used for each technology. BmC was determined for each technology dataset ranging from 0.41-0.5 kg C kg^{-1} biomass DM in Andrade et al..

Cc is a parameter fed to AMG that allows determining the C input based on the crop yields. Cc was used in Eq (S2) to determine the amount of C from a given co-product that would be applied in a given simulation unit per year.

$$TBpC = Wt(dm)_i * WtCc_i * Cc \qquad \text{(Eq S2)}$$

where TBpC is the total coproduct C applied [t C ha^{-1} y^{-1}], $Wt(dm)_i$ is the crop residues mass available for crop i [t crop residues ha^{-1} y^{-1}], $WtCc_i$ is the Crop residue carbon content for crop residue i [t C t^{-1} crop]. The suffix i denotes the different crops that could be included in the rotation. AMG follows an annual timestep, therefore, it allows to input only one main crop per year.

184 $Wt(dm)_i$ is determined for each crop in each simulation unit based on the HI and allocation
185 coefficients (Bolinder et al., 2007) and the grain yield [t biomass DM ha^{-1} y^{-1}] input, while WtCCi
186 was defined as 0.444 g C g^{-1} biomass DM (Clivot et al., 2019).

187 ***2.2 AMG adaptation: Carbon Recalcitrance (Cr) of bioeconomy coproducts***

188 The soil carbon partitioning in AMG is described by Eq S3 and Eq S4 (Clivot et al., 2019).

189 $$QC = QC_S + QC_A \qquad \text{(Eq S3)}$$

190 $$\frac{dQC_A}{dt} = \sum_i m_i h_i - kQC_A \qquad \text{(Eq S4)}$$

191 where *QC* is the total SOC stock (t ha^{-1}), QC_A and QC_S are the C stocks of the active and stable C
192 pools (t ha^{-1}) respectively, m_i is the annual C input from organic residue *i* (t ha^{-1} yr^{-1}), *h* is its
193 humification or retention coefficient and *k* is the mineralization rate constant of the active C
194 pool (yr^{-1}).

195 The bioeconomy co-products are assumed to be composed of two carbon fractions, one called
196 labile, and another known as stable or recalcitrant. The labile fraction is easily mineralizable as
197 CO_2 while the recalcitrant fraction is less prone to degradation and is mineralized at a slower
198 rate than the former one. The size (%) of each fraction and the time of residence in the soil of
199 the recalcitrant one varies for each co-product in function of the technology conditions.

200 For the less recalcitrant coproducts (digestate, hydrochar, molasses) the labile fraction has sizes
201 around 20 – 50%, while the recalcitrant fraction of this group tends to exhibit MRT values lower
202 than 26 years which are values considered to be close to the MRT of the active pool. Thus, for
203 this group of products the fraction remaining after one year (*h*) is considered to correspond to
204 the recalcitrant fraction defined by the coefficient Cr. Therefore, Cr is defined as the active
205 retention coefficient (h_a) and is completely allocated in the active pool C_A where it will be slowly
206 mineralized.

The recalcitrant fraction of the highly recalcitrant co-products (pyrochar and gaschar) constitutes 95% of the coproduct total carbon and exhibit MRTs longer than the 100 years of simulation conducted here, thus they were treated by way of simplification as inert in our modeling approach. For this group, the adapted AMG version considered that the recalcitrant fraction determined by Cr is directly allocated in the C_S pool of the model as the stable retention coefficient (h_s). The labile fraction (5%) is considered to be readily mineralized at the annual time-step.

5. Sensitivity Analyses (SA)

Based on the range of Cc and Cr values reported on (Review), an average result was obtained for the distinct types of feedstocks considered for a given technology. Then the first and third quartiles were selected as a low and a high value, respectively, to be tested in the SA. This approach permitted testing the range of values observed, while not being influenced by the less- likely- to- happen extreme values. This approach resulted in three levels for each parameter.

The "main scenarios" for each technology consisted of the combination of the average values of each parameter (Cc_{mean} – Cr_{mean}). The SA constituted new scenarios, which considered the different possible combinations between the two coefficients and the three levels. Combining a mean value with a low or high value would allow identifying the sensitivity of the model to the change in the parameter modified as low or high (i.e., Cc_{mean}-Cr_{high} allows to identify the effect of Cr). The combinations between low and high values allowed to identify the combined effect of changing both parameters (i.e., Cc_{low}-Cr_{low}, Cc_{low}-Cr_{high}, etc.)

The way of determining Cr plays a role in the modeled SOC evolution. We considered this source of uncertainty by calculating C_S under two different methods for the pyrolysis scenario.

In the **first method,** as explained in the main body, section 2.3.3, we considered that the recalcitrant fraction would be allocated directly in the C_S pool, and we assumed that nothing would be allocated in the active pool C_A.

Various modeling assays linked to laboratory incubations and field trials have determined that the recalcitrant fraction would not be inert but would follow a very little decay rate. Therefore, in the **second method**, we determined the amount of C mineralized during the first year based on incubation assays lasting less than 1 year. It was noted that 80% of the labile fraction (5%) would be mineralized in the first couple of months and the other 20% would have a mean life of 10 years (Lehmann and Joseph, 2010). In that sense, 4% of the biochar would be directly mineralized in the first year and 1% is allocated in the C_A pool to be slowly mineralized.

The C lost in 100 years has been determined by various authors for different crop residues-based biochar (Hammes et al., 2008; Herath et al., 2015; Zimmerman, 2010) using Eq S5 (Lehmann et al., 2015).

$$M_t = M_1\left(1 - e^{-k_1 t}\right) + M_2\left(1 - e^{-k_2 t}\right) \qquad \text{(Eq S5)}$$

where Mt is the Carbon mineralized in mg C g^{-1} biochar at time t, M_1 is the labile mineralizable fraction, M_2 is the recalcitrant C fraction, and k_1 and k_2 are the first-order degradation rate constants for the labile and recalcitrant pools, respectively.

Mean values of 26% C lost in 100 years have been obtained in Andrade et al. from the studies calculating it. This value falls under IPCC (2019) guidelines, which suggest that 80% (±11%) of biochar (pyrolysis, 450-600°C) remains after 100 years. Although evidence suggests that biochar losses in a century could be significantly lower (Zimmerman and Gao, 2013) and the MRT obtained from the ensemble of works in Andrade et al. at pyrolysis temperatures of 300 – 500°C is 812 years, we opt to be conservative. Therefore, we defined that 75% of pyrochar is inert during the 100 years of modeling and is allocated in the C_S pool as the h_s coefficient. After

considering the losses in the first year (*1-h_s*), the labile fraction, and the inert fraction (100 years), the h_a coefficient was calculated to be 0.21 using Eq S6.

$$h_{a\_pyro} = 1 - (80\%)(C_L) - h_S \qquad \text{Eq S6}$$

where h_{a_pyro} is the active retention coefficient for the pyrochar scenario alternative method, C_L is the labile fraction of pyrochar (5%) and h_S is the stable pool corresponding to the inert fraction of pyrochar for 100 years (75%).

As done for the first method, we investigated three levels of h_a and h_S, based on the mean value and the first and third quartile presented in Andrade et al.. The combination of "main scenarios" and "SA scenarios" yielded a total of 54 scenarios explored (Table SI2).

Table S1.2. -Different combinations of parameters considered for sensitivity. The Cr has been split between h_a and h_S

Bioeconomy pathways	**Recalcitrance (Cr)**						**(Cc)**		
	ha			**h_S**					
	Low	**Mean**	**High**	**Low**	**Mean**	**High**	**Low**	**Mean**	**High**
Pyrochar[a]	n/a	n/a	n/a	90	95	99	34	44	54
Pyrochar[b]	36	21	7	60	75	89	34	44	54
Gaschar	n/a	n/a	n/a	90	95	99	14	20	25
Hydrochar	80	83	96	n/a	n/a	n/a	12	31	45
Digestate	58	68	77	n/a	n/a	n/a	29	39	49
Lignocellulosic ethanol molasses	28	45	60	n/a	n/a	n/a	18	24	30

Cr : Carbon recalcitrance, h_a : retention coefficient in the active pool, h_s : retention coefficient in the stable pool, Cc : Carbon conversion

[a] First method of introducing Cr for inert fractions in AMG

[b] Second method of introducing Cr for inert fractions in AMG

n/a under h denotes that the C_A pool was not considered in the model while under C_S denotes that the C_S pool was not considered in the model.

A total of 9 extra SA tests were performed to assess the effects of limiting the pyrochar and gaschar application rate and decreasing the exporting rate when SOC losses were observed (AD, HTL, and 2G Ethanol production scenarios).

SA Result Figures

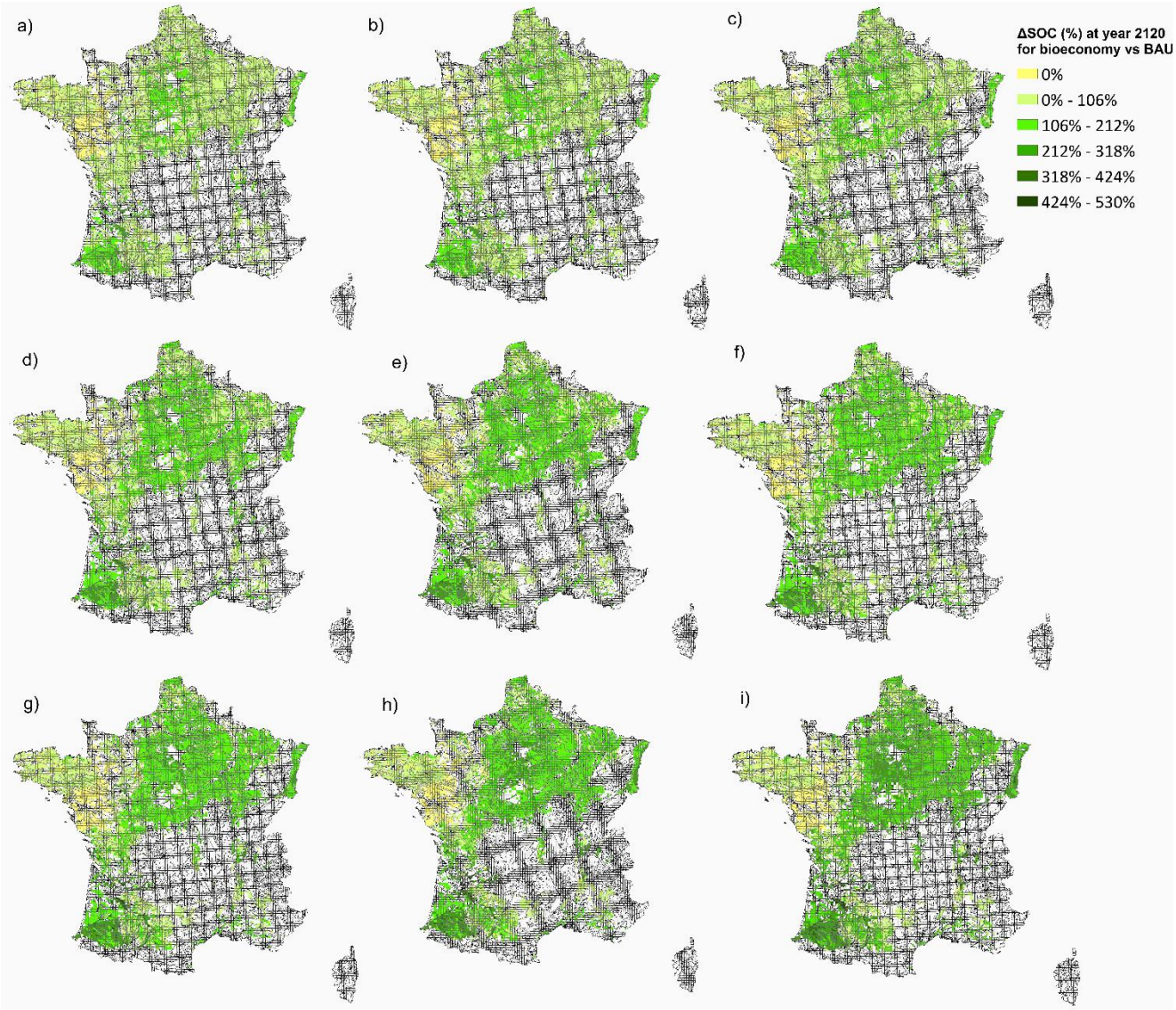

Fig. S4. Sensitivity analyses (SA) for the pyrolysis scenario determined without the active pool: a) LL: Low Cc – Low Cr, b) LM: Low Cc – Mean Cr, c) LH: Low Cc- High Cr, d) ML: Mean Cc – Low

Cr, e) MM: Mean Cc – Mean Cr (Main scenario), f) MH: Mean Cc – High Cr, g) HL: High Cc – Low Cr, g) HM: High Cc – Mean Cr, i) HH: High Cc – High Cr

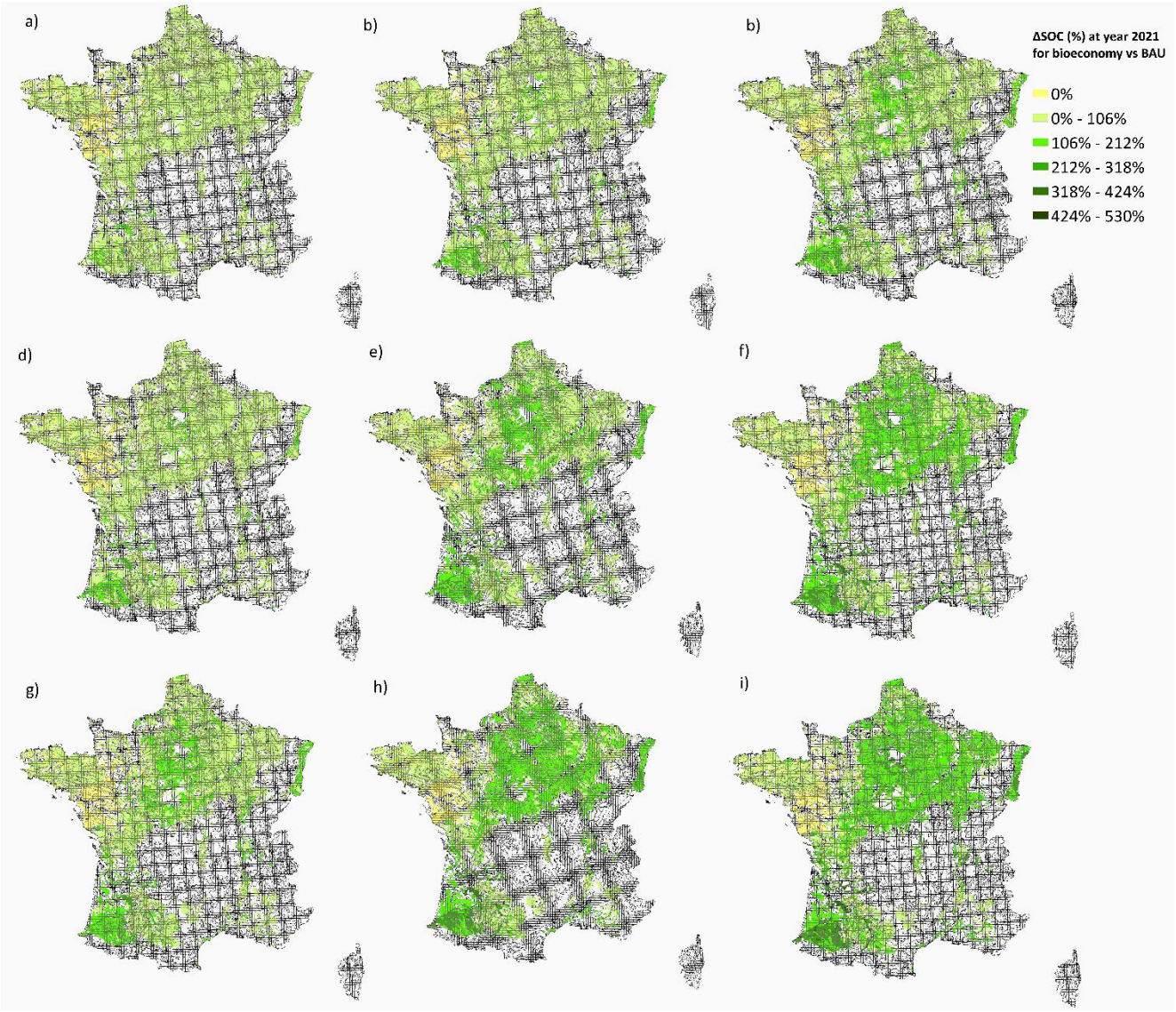

Fig. S5. Sensitivity analyses (SA) for the pyrolysis scenario determined with the active and stable pools: a) LL: Low Cc – Low Cr, b) LM: Low Cc – Mean Cr, c) LH: Low Cc- High Cr, d) ML: Mean Cc – Low Cr, e) MM: Mean Cc – Mean Cr (Main scenario), f) MH: Mean Cc – High Cr, g) HL: High Cc – Low Cr, g) HM: High Cc – Mean Cr, i) HH: High Cc – High Cr

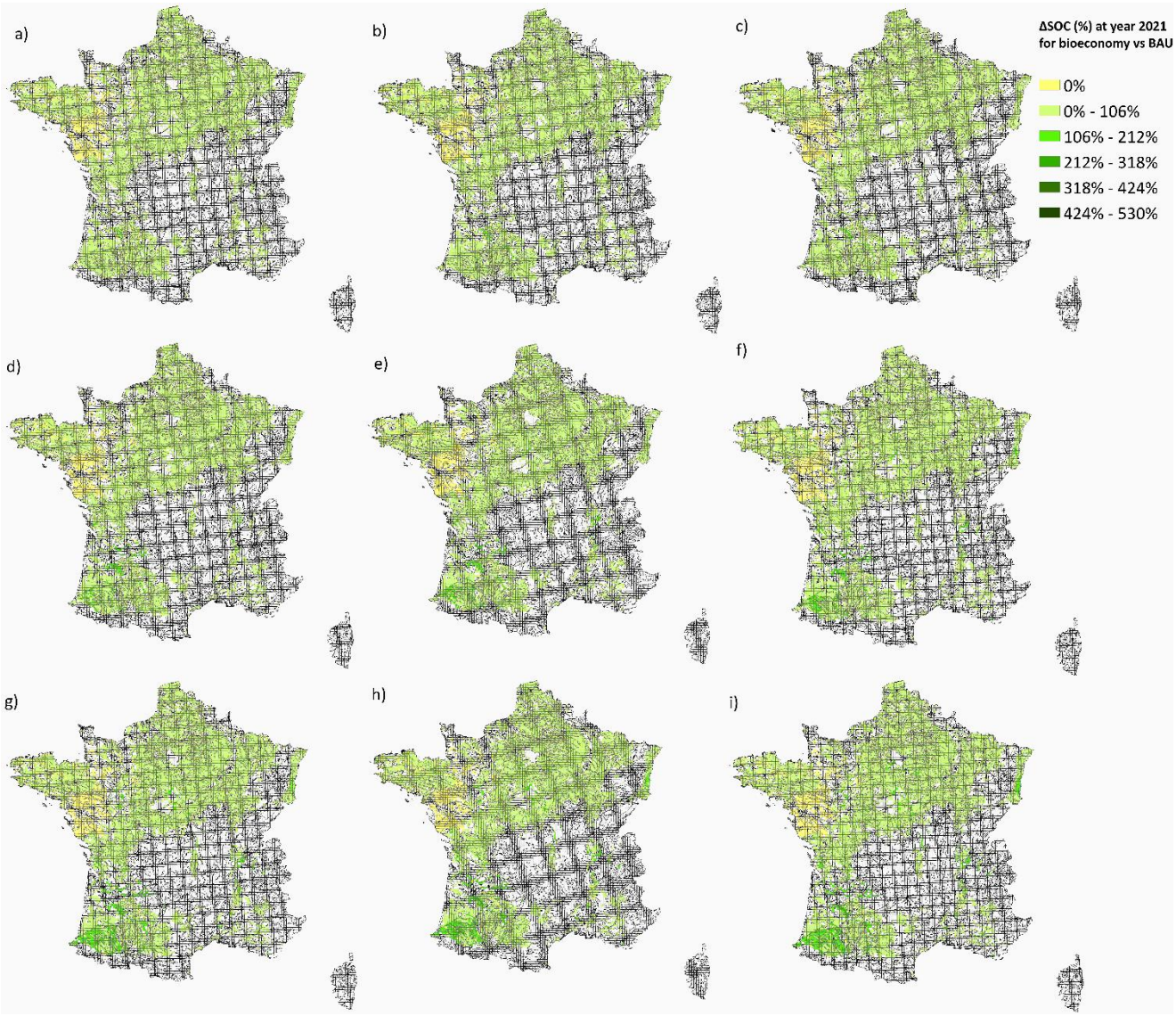

Fig. S6. Sensitivity analyses (SA) for the gasification scenario: a) LL: Low Cc – Low Cr, b) LM: Low Cc – Mean Cr, c) LH: Low Cc- High Cr, d) ML: Mean Cc – Low Cr, e) MM: Mean Cc – Mean Cr (Main scenario), f) MH: Mean Cc – High Cr, g) HL: High Cc – Low Cr, g) HM: High Cc – Mean Cr, i) HH: High Cc – High Cr

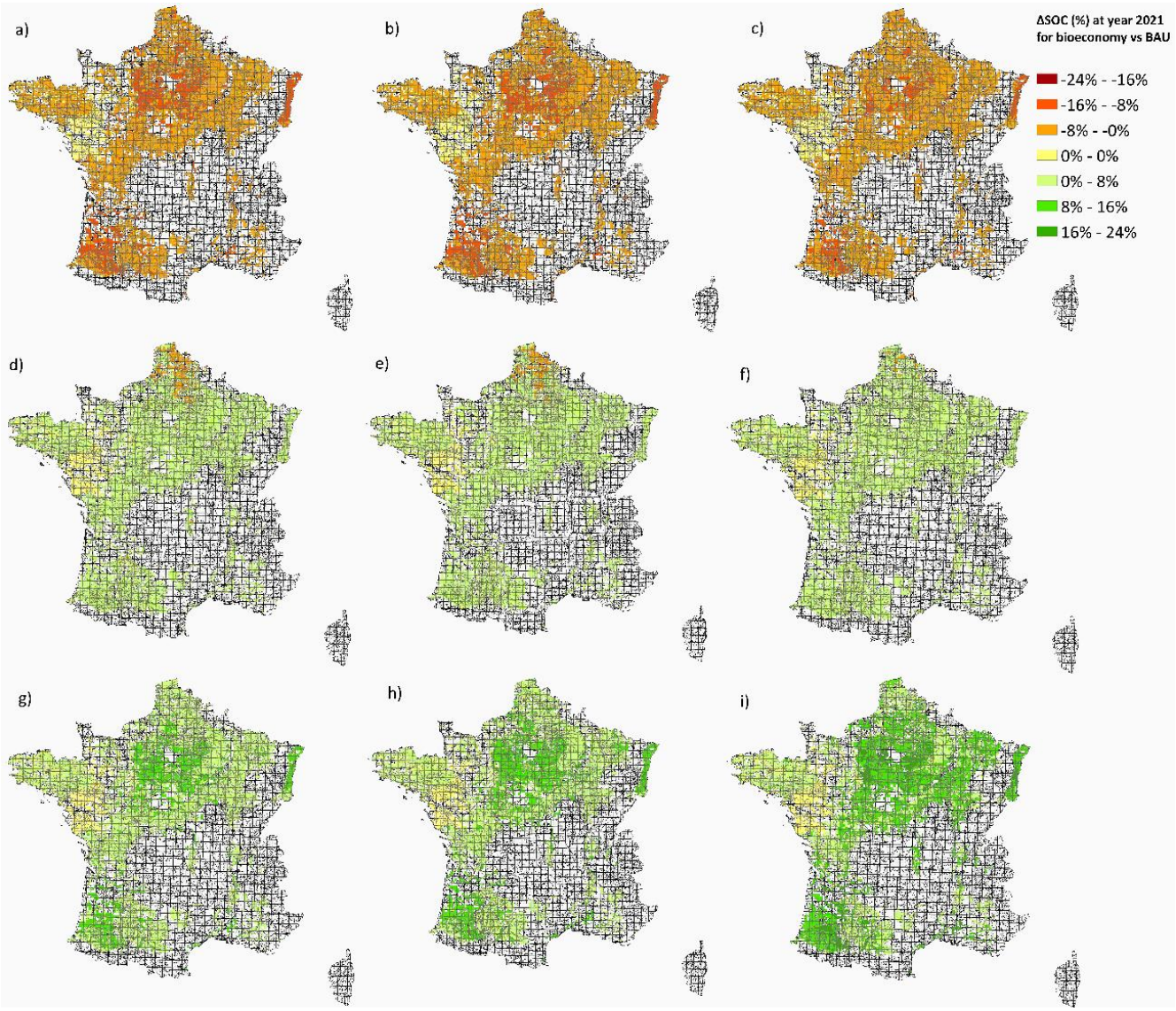

Fig. S7. Sensitivity analyses (SA) for the hydrothermal liquefaction scenario: a) LL: Low Cc – Low Cr, b) LM: Low Cc – Mean Cr, c) LH: Low Cc- High Cr, d) ML: Mean Cc – Low Cr, e) MM: Mean Cc – Mean Cr (Main scenario), f) MH: Mean Cc – High Cr, g) HL: High Cc – Low Cr, g) HM: High Cc – Mean Cr, i) HH: High Cc – High Cr

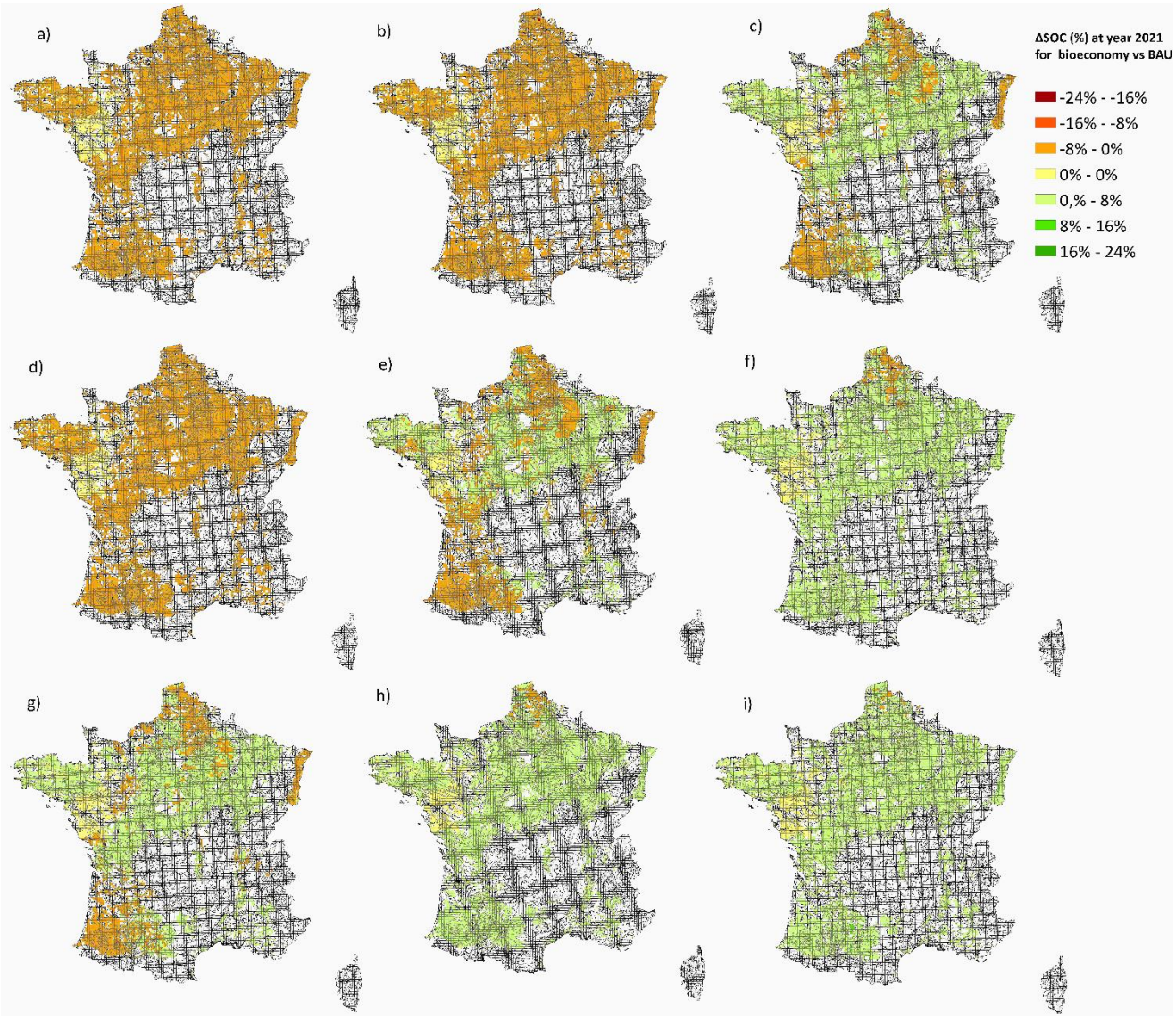

Fig. S8. Sensitivity analyses (SA) for the anaerobic digestion scenario: a) LL: Low Cc – Low Cr, b) LM: Low Cc – Mean Cr, c) LH: Low Cc- High Cr, d) ML: Mean Cc – Low Cr, e) MM: Mean Cc – Mean Cr (Main scenario), f) MH: Mean Cc – High Cr, g) HL: High Cc – Low Cr, g) HM: High Cc – Mean Cr, i) HH: High Cc – High Cr

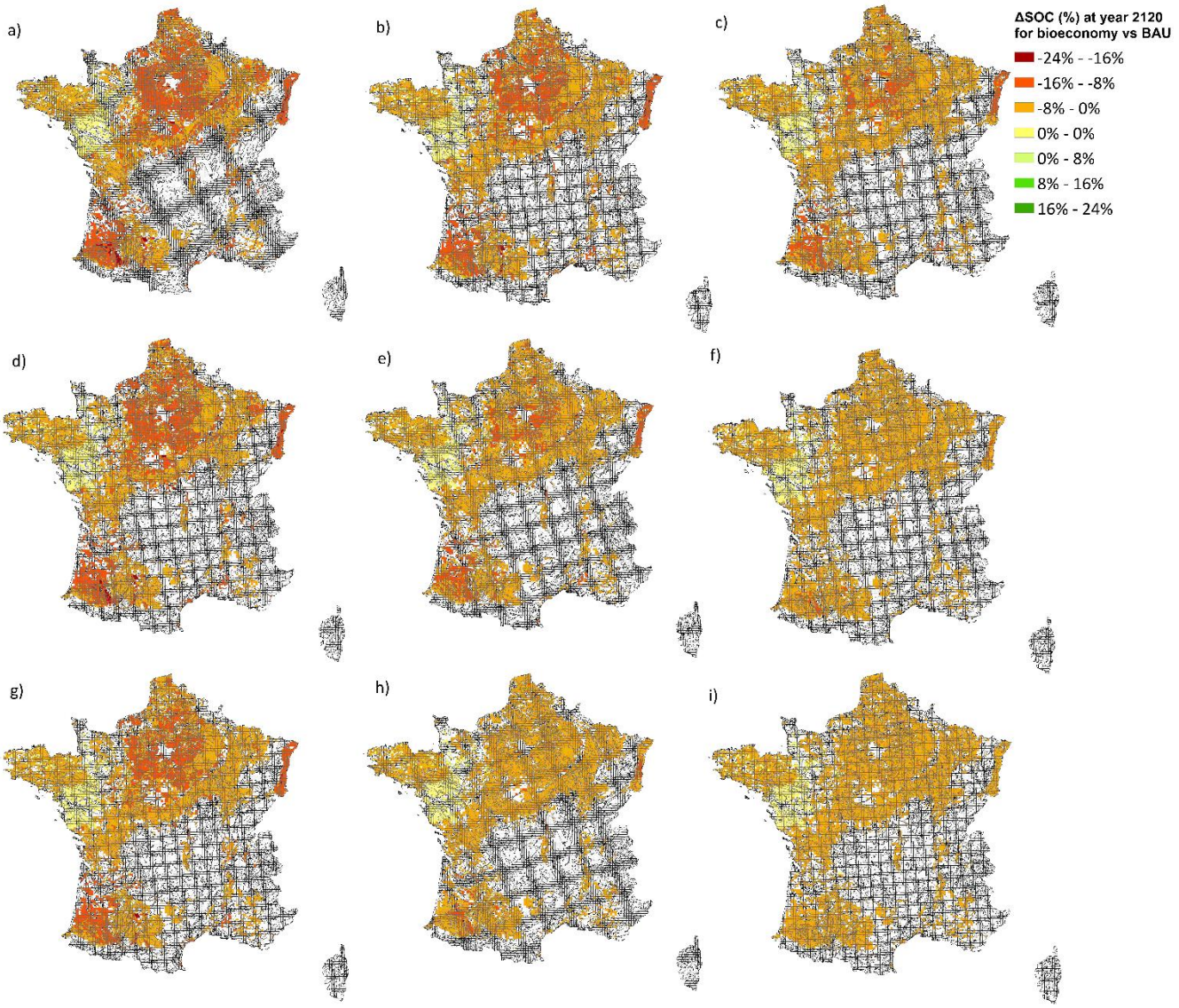

306

307 Fig. S9. Sensitivity analyses (SA) for the lignocellulosic ethanol scenario: a) LL: Low Cc – Low Cr,

308 b) LM: Low Cc – Mean Cr, c) LH: Low Cc- High Cr, d) ML: Mean Cc – Low Cr, e) MM: Mean Cc –

309 Mean Cr (Main scenario), f) MH: Mean Cc – High Cr, g) HL: High Cc – Low Cr, g) HM: High Cc –

310 Mean Cr, i) HH: High Cc – High Cr

311 **References**

312 Bolinder, M.A., Janzen, H.H., Gregorich, E.G., Angers, D.A., VandenBygaart, A.J., 2007. An
313 approach for estimating net primary productivity and annual carbon inputs to soil for
314 common agricultural crops in Canada. Agriculture, Ecosystems & Environment 118,
315 29–42. https://doi.org/10.1016/j.agee.2006.05.013
316 Bušić, A., 2018. Bioethanol Production from Renewable Raw Materials and Its Separation and
317 Purification: A Review 56, 23.
318 Clivot, H., Mouny, J.-C., Duparque, A., Dinh, J.-L., Denoroy, P., Houot, S., Vertès, F., Trochard,
319 R., Bouthier, A., Sagot, S., Mary, B., 2019. Modeling soil organic carbon evolution in
320 long-term arable experiments with AMG model. Environmental Modelling & Software
321 118, 99–113. https://doi.org/10.1016/j.envsoft.2019.04.004
322 GisSol, 2011. La texture dominante de l'horizon supérieur des sols agricoles par canton [WWW
323 Document].
324 Hammes, K., Torn, M.S., Lapenas, A.G., Schmidt, M.W.I., 2008. Centennial black carbon
325 turnover observed in a Russian steppe soil. Biogeosciences 5, 1339–1350.
326 https://doi.org/10.5194/bg-5-1339-2008
327 Herath, H.M.S.K., Camps-Arbestain, M., Hedley, M.J., Kirschbaum, M.U.F., Wang, T., van Hale,
328 R., 2015. Experimental evidence for sequestering C with biochar by avoidance of CO_2
329 emissions from original feedstock and protection of native soil organic matter. GCB
330 Bioenergy 7, 512–526. https://doi.org/10.1111/gcbb.12183
331 IPCC, 2019. 2019 Refinement to the 2006 IPCC Guidelines for National Greenhouse Gas
332 Inventories - Appendix4: Method for Estimating the Change in Mineral Soil Organic
333 Carbon Stocks from Biochar Amendments: Basis for Future Methodological
334 Development. IPCC.

335 Jahirul, M., Rasul, M., Chowdhury, A., Ashwath, N., 2012. Biofuels Production through Biomass
336 Pyrolysis —A Technological Review. Energies 5, 4952–5001.
337 https://doi.org/10.3390/en5124952
338 Joly, D., Brossard, T., Cardot, H., Cavailhes, J., Hilal, M., Wavresky, P., 2010. Les types de climats
339 en France, une construction spatiale. Cybergeo : European Journal of Geography [En
340 ligne], Cartographie, Imagerie, SIG. https://doi.org/10.4000/cybergeo.23155
341 Launay, C., Constantin, J., Chlebowski, F., Houot, S., Graux, A., Klumpp, K., Martin, R., Mary, B.,
342 Pellerin, S., Therond, O., 2021. Estimating the carbon storage potential and
343 greenhouse gas emissions of French arable cropland using high-resolution modeling.
344 Glob. Change Biol. 27, 1645–1661. https://doi.org/10.1111/gcb.15512
345 Lehmann, J., Abiven, S., Kleber, M., Pan, G., Singh, B.P., Sohi, S.P., Zimmerman, A.R., 2015.
346 Persistence of biochar in soil, in: Biochar for Environmental Management. p. 48.
347 Lehmann, J., Joseph, S. (Eds.), 2010. Biochar for environmental management: science and
348 technology, Reprint. ed. Earthscan, London.
349 Malyan, S.K., Kumar, S.S., Fagodiya, R.K., Ghosh, P., Kumar, A., Singh, R., Singh, L., 2021.
350 Biochar for environmental sustainability in the energy-water-agroecosystem nexus.
351 Renewable and Sustainable Energy Reviews 149, 111379.
352 https://doi.org/10.1016/j.rser.2021.111379
353 Molino, A., Chianese, S., Musmarra, D., 2016. Biomass gasification technology: The state of the
354 art overview. Journal of Energy Chemistry 25, 10–25.
355 https://doi.org/10.1016/j.jechem.2015.11.005
356 Seehar, T.H., Toor, S.S., Sharma, K., Nielsen, A.H., Pedersen, T.H., Rosendahl, L.A., 2021.
357 Influence of process conditions on hydrothermal liquefaction of eucalyptus biomass
358 for biocrude production and investigation of the inorganics distribution. Sustainable
359 Energy Fuels 5, 1477–1487. https://doi.org/10.1039/D0SE01634A

Swain, M.R., Singh, A., Sharma, A.K., Tuli, D.K., 2019. Chapter 11 - Bioethanol Production From Rice- and Wheat Straw: An Overview, in: Bioethanol Production from Food Crops. Sustainable Sources, Interventions, and Challenges. Academic Press, p. 19.

Tonini, D., Hamelin, L., Astrup, T.F., 2016. Environmental implications of the use of agro-industrial residues for biorefineries: application of a deterministic model for indirect land-use changes. GCB Bioenergy 8, 690–706. https://doi.org/10.1111/gcbb.12290

Zimmerman, A., Gao, B., 2013. The Stability of Biochar in the Environment, in: Ladygina, N., Rineau, F. (Eds.), Biochar and Soil Biota. CRC Press, pp. 1–40. https://doi.org/10.1201/b14585-2

Zimmerman, A.R., 2010. Abiotic and Microbial Oxidation of Laboratory-Produced Black Carbon (Biochar). Environ. Sci. Technol. 44, 1295–1301. https://doi.org/10.1021/es903140c